

<https://doi.org/10.1038/s41523-025-00734-x>

# Development and validation of a functional ex vivo paclitaxel and eribulin sensitivity assay for breast cancer, the REMIT assay

Check for updates

Zofia M. Komar<sup>1</sup>, Nicole S. Verkaik<sup>1,2</sup>, Ahmed Dahmani<sup>3</sup>, Elodie Montaudon<sup>3</sup>, Roland Kanaar<sup>1,2</sup>,  
Adriaan B. Houtsmuller<sup>4</sup>, Agnes Jager<sup>5</sup>, Elisabetta Marangoni<sup>3</sup> & Dik C. van Gent<sup>1,2</sup> ✉

Breast cancer is the most common cancer amongst women worldwide, however clinically validated chemotherapy response biomarkers that can accurately predict treatment response in patients are largely lacking. Therefore, in this study, functional paclitaxel and eribulin ex vivo sensitivity assays were developed. Patient derived xenograft (PDX) models were used to compare the ex vivo predicted treatment outcome with the sensitivity of mice in vivo. We validated the previously developed sensitivity assay for paclitaxel, which is based on the ratio between replicating (EdU) and mitotic (phospho-Histone H3; pH3) cells as a proxy for blocked mitosis. The assay showed 90% correlation between the ex vivo and in vivo response to paclitaxel treatment in the PDX models. We propose the term REMIT (REplication MITosis) assay and show that it is also a suitable test to predict eribulin sensitivity. The reproducibility of the REMIT assay for paclitaxel and eribulin was determined to be 80% and 83%, respectively. These results justify further clinical validation of the REMIT assay in breast cancer patients.

Breast cancer (BC) is the most prevalent cancer among women worldwide<sup>1</sup>. Despite extensive research and advancements in diagnostics, selecting the optimal therapy for BC remains a challenge due to the high heterogeneity. BC can be categorized based on the expression of estrogen receptor (ER), progesterone receptor (PR), and human epidermal growth factor receptor 2 (HER2)<sup>2</sup>. Targeted treatments, including hormonal therapies and anti-HER2 treatment, have proven successful for tumors expressing PR, ER or HER2 receptors<sup>3</sup>. Triple-negative breast cancers (TNBCs), constituting approximately 10–20% of all BCs, lack expression of these surface receptors, however much improvement has been made to also improve therapy options for these patients<sup>4,5</sup>. Regardless of the progress made in the development of targeted treatment options, the therapy with cytotoxic drugs still remains the backbone of BC treatment. Unfortunately, not all patients benefit from chemotherapy, with 30% of TNBC patients that achieve full response after the treatment<sup>6</sup>. Common chemotherapy regimens for BC treatment involve anthracyclines (e.g. doxorubicin), taxanes (e.g. paclitaxel), alkylating agents (e.g. cyclophosphamide), antimetabolites (capecitabine), platinum agents (e.g. carboplatin) and microtubule inhibitors (e.g. eribulin), and combinations of these agents<sup>7,8</sup>. However, the lack of validated predictive biomarkers hampers the ability to predict the most effective

chemotherapy for individual patients. Current research to find predictive biomarkers for BC treatment relies on gene and protein expression in cancer cells<sup>9</sup>, which aid in categorizing patients into risk groups but fall short in predicting chemotherapy responses.

To address the critical need for developing robust predictive biomarkers for response to chemotherapies, our previous work focused on the development of functional ex vivo assays to predict response to anthracycline<sup>10</sup>, cisplatin and docetaxel treatments<sup>11</sup>. Generally, these assays are developed in the pre-clinical setting and further clinically validated. Recognizing the growing demand for alternative assays in a clinical setting, we expand our research to eventually develop functional ex vivo tests for all clinically available chemotherapy regimens. In this study, the functional ex vivo test for two microtubule targeting agents (MTAs) with distinct mechanisms of action was developed and validated pre-clinically.

Taxanes (paclitaxel and docetaxel) are the most widely used taxane-based chemotherapies commonly employed in various cancer treatments, including breast cancer<sup>12</sup>. These drugs, effectively inhibit cancer cell proliferation by obstructing the process of mitosis<sup>13,14</sup>. Paclitaxel is able to bind to  $\beta$ -tubulin, thereby blocking the ability of microtubules to either grow or shorten<sup>15</sup>. Another MTA drug used in a clinical setting is eribulin. This

<sup>1</sup>Department of Molecular Genetics, Erasmus MC Cancer Institute, Rotterdam, The Netherlands. <sup>2</sup>Oncode Institute, Erasmus MC, Rotterdam, The Netherlands.

<sup>3</sup>Translational Research Department, Institut Curie, PSL University, Paris, France. <sup>4</sup>Erasmus Optical Imaging Center and Department of Pathology, Erasmus MC, Rotterdam, The Netherlands. <sup>5</sup>Department of Medical Oncology, Erasmus MC Cancer Institute, Rotterdam, The Netherlands. ✉e-mail: [d.vangent@erasmusmc.nl](mailto:d.vangent@erasmusmc.nl)

FDA-approved chemotherapeutic, is utilized for patients with metastatic BC who have previously undergone anthracycline and taxane treatments<sup>16</sup>. Eribulin is a drug affecting cell division by inhibiting microtubule dynamics<sup>17</sup>. In contrast to other MTAs, eribulin affects only the growth of microtubules, leading to inhibition of mitotic spindle assembly during prometaphase<sup>18</sup>. However, not all patients respond to these treatments, making the development of sensitivity assays based on specific tumor features of high importance.

Our current study aims to develop the ex vivo functional sensitivity assays for paclitaxel and eribulin and validate these assays in mice in vivo. We first applied the docetaxel sensitivity assay developed by Ladan et al.<sup>11</sup> for paclitaxel and termed it the REMIT (REplication MITosis) assay. Next, the REMIT assay was validated for paclitaxel sensitivity testing by comparing the ex vivo sensitivity and the in vivo response in ten different mouse PDX models. Similarly, the REMIT assay was selected for eribulin-sensitivity assessment and validated by comparing the ex vivo sensitivity with the in vivo response of a representative PDX model.

## Results

### Paclitaxel treatment does not lead to direct tumor killing ex vivo

We previously observed that docetaxel treatment ex vivo did not lead to tumor death in primary tumors<sup>11</sup>. To investigate the response to paclitaxel treatment, ten different BC PDX models with known sensitivity to paclitaxel were tested in triplicate (Fig. 1). The relative number of replicating cells and cells in apoptosis, respectively, were determined after treatment with increasing concentrations of paclitaxel (1, 3, 6, 10, 18, 25 and 100 nM) for three days. In all ten tested PDX models, cancer cells continued to replicate after three days of paclitaxel treatment (Fig. 1a–d; Supplementary Fig. 2). No clear decline in cell replication that could be correlated with the known in vivo sensitivity was observed. Similarly, the levels of apoptosis after paclitaxel treatment based on the TUNEL assay did not show a clear induction of apoptosis in any of the models (Fig. 1e–h; supplementary Fig. 3). In some models, a slight induction of apoptosis was observed at higher concentrations of the treatment (e.g. HBCx-204), but this did not correlate with the known paclitaxel sensitivity in vivo nor to the ex vivo tested replication levels. Overall, paclitaxel treatment did not result in a specific decline in replication nor induction of apoptosis in all seven in vivo paclitaxel-sensitive models, confirming that paclitaxel treatment ex vivo for three days does not lead to direct tumor killing.

### Paclitaxel sensitivity can be assessed by the REMIT assay

As paclitaxel did not affect the viability of the BC PDX models, we developed an alternative method – the REMIT assay. Paclitaxel affects microtubules and interferes with mitosis<sup>19</sup>. Therefore, we investigated the relative number of cells in mitosis (pH3) within a tissue slice with and without paclitaxel treatment, as previously described for docetaxel treatment<sup>11</sup>, by calculating the ratio, defined as the number of replicating (EdU-positive) cells divided by the number of pH3-positive cells. As expected, paclitaxel treatment resulted in an increase of the relative number of cells arrested in mitosis (Fig. 2a). The EdU/pH3 ratio declined when compared to the untreated sample in paclitaxel-sensitive (e.g. HBCx-4B), but not in resistant (e.g. HBCx-39) PDX tumors at a relatively low paclitaxel concentration (Fig. 2b and c), indicating that in sensitive tumor cells the cell cycle is blocked in mitosis. To set appropriate thresholds for sensitivity assessment, the results of the EdU/pH3 ratio for all tested PDX models were combined. The relative EdU/pH3 was calculated by comparing the treated EdU/pH3 levels with the untreated control. Based on the ex vivo data, ten tested PDX models were categorized into ex vivo paclitaxel sensitive and resistant tumors, respectively. The cut-off relative EdU/pH3 value at 10 nM of paclitaxel, chosen to be the most discriminating, was 45%, with values above 45% considered resistant and below sensitive (Fig. 2d). To compare the ex vivo predicted paclitaxel sensitivity with the in vivo sensitivity of these tumors tested in mice, the tumor growth inhibition was determined for each of the models, separately (Supplementary Fig. 4). Based on the TGI values the models were categorized between in vivo sensitive and resistant tumors (Fig. 2e). The ex vivo

and in vivo sensitivity to paclitaxel was compared, and the concordance between the predictive paclitaxel ex vivo assay with the known in vivo response was determined to be 90% (Fig. 2f). One out of the ten tested BC PDX models (HBCx-216) showed sensitivity to paclitaxel in vivo, but resistance ex vivo. This assay has previously been developed using clinical material for docetaxel sensitivity<sup>11</sup>. Additionally, a group of primary tumors has been tested in this study for paclitaxel sensitivity using the REMIT assay (see supplementary Fig. 5), showing that this assay also works on clinical material.

### Eribulin treatment ex vivo lowers replication rate but does not induce apoptosis

To extend the ex vivo assay we aimed to develop an eribulin-sensitivity assay using the BC PDX models. For this purpose, the ten PDX models used for paclitaxel assay development were treated for three days with a range of eribulin concentrations. To find the most optimal read-out for eribulin sensitivity the levels of replication (EdU), apoptosis (TUNEL) and mitosis (pH3) were analyzed after treatment. Again, no clear decline in replication after eribulin treatment was observed in six of the models (Fig. 3; supplementary Fig. 2c). In contrast to paclitaxel, eribulin treatment resulted in a decline in replication in four of the tested models (Fig. 3a–c). A significant decrease in replication was observed for HBCx-204 (37%) and HBCx-4B (75%) at 3 nM, for HBCx-137 (27%) at 1 nM eribulin; and for HBCx-11 (71%) at 25 nM. Two models (HBCx-209 and HBCx-147) showed a significant decline in replication at 10 nM, but the levels increased again at higher concentrations, suggesting the influence of heterogeneity between slices rather than a specific effect on cell viability (Supplementary Fig. 2c). To determine whether the observed decline in replication in HBCx-204, HBCx-4B, HBCx-137 or HBCx-11 was related to direct tumor killing, the TUNEL assay was performed to measure the levels of apoptosis (Fig. 3d–f). Overall, no significant differences in the levels of apoptosis were observed after eribulin treatment in the tested PDX models. In conclusion, no clear effect of eribulin treatment on cell viability was observed that could be applied to use the EdU and TUNEL assays for sensitivity assessment. This shows that, similarly to paclitaxel, three-day eribulin treatment ex vivo does not lead to direct tumor killing.

### Eribulin sensitivity can be predicted by the REMIT assay in treated tissue slices

Similarly to paclitaxel treatment, the decline in replication observed after eribulin treatment ex vivo did not show sufficient differences among the tested models to develop a sensitive ex vivo assay. Combined with a lack of apoptosis induction, we conclude that an alternative read-out will be more promising to assess eribulin sensitivity. Therefore, like for paclitaxel treatment, the REMIT assay was selected to assess whether inhibition of mitosis (a decrease in EdU/pH3 ratio) might be a suitable read-out. BC PDX tissue slices were treated with eribulin for three days after which the levels of the EdU/pH3 ratio were investigated in all ten BC PDX models (Fig. 4). The in vivo sensitivity to eribulin was tested only for the HBCx-137 model, showing its sensitivity to the treatment (Fig. 4c). This model was considered representative for eribulin sensitivity. The ratio between the number of EdU- and pH3-positive cells was calculated and normalized by calculating the percentage of the ratio after treatment relative to the control. Each model was plotted separately to apply appropriate thresholds (Fig. 4a, b). Based on the response of the HBCx-137 to eribulin treatment, the concentration of 1 nM of eribulin was selected as the most optimal to distinguish between eribulin sensitive and resistant models (Fig. 4b). Samples that showed the normalized EdU/pH3 value above 45% after treatment with 1 nM eribulin were considered resistant and below 45% sensitive. Considering, that eribulin treatment has been shown effective for treatment of a fraction of the paclitaxel-sensitive patients<sup>20</sup>, we investigated whether any correlation can be seen between the sensitivity to paclitaxel and eribulin ex vivo. Here we show, that seven of the tested models displayed the same sensitivity to paclitaxel and eribulin treatment based on the REMIT assay (Fig. 4d). Models HBCx-11 and HBCx-3 showed differences between treatments with

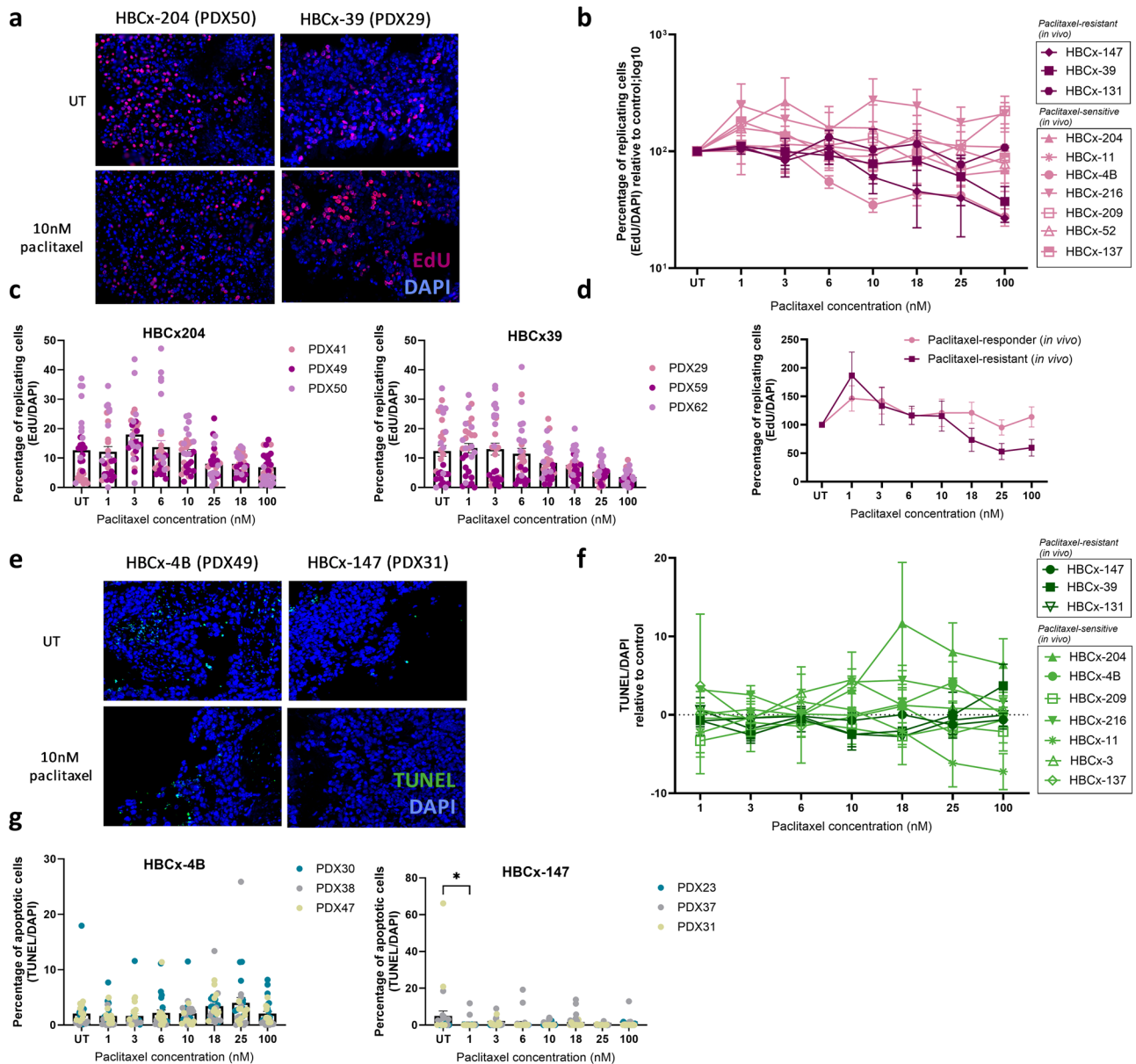


**Fig. 1 | Viability assessment of the PDX tumor tissue after paclitaxel treatment.** **a** Representative images of the EdU (pink) and DAPI (blue) channels for two selected PDX models: HBCx-204 and HBCx-39. **b** Combined EdU/DAPI results for each model separately relative to the control, with mean and SEM indicated. **c** EdU/DAPI replication results after paclitaxel treatment of two selected PDX models (HBCx-204 and HBCx-39). Each data point represents the percentage of replicating cells within one microscopic field of view; ten fields of view were analyzed for each of the three biological replicates. **d** Combined EdU/DAPI results divided in paclitaxel sensitive

and resistant models. **e** Representative images of the TUNEL (green) and DAPI (blue) channels for two selected PDX models: HBCx-4B and HBCx-147. **f** Combined TUNEL/DAPI results for each model separately relative to the control by subtracting it from the TUNEL levels after treatment. Error bars represent the SEM. **g** TUNEL/DAPI replication results after treatment with paclitaxel of two selected PDX models (HBCx-4B and HBCx-147). Each data point represents the percentage of replicating cells within one microscopic field of view; ten fields of view were analyzed for each of the three biological replicates.

sensitivity to paclitaxel and resistance to eribulin. Model HBCx-131 reacted resistant to paclitaxel treatment ex vivo and in vivo, however it showed sensitivity to eribulin.

**The REMIT assay is a sensitive and reproducible method for the assessment of paclitaxel and eribulin sensitivity**

We analyzed the reproducibility of the REMIT assay for paclitaxel and eribulin sensitivity, to determine whether both assays are potentially suitable for clinical application. For that purpose, the individual replicates of the tested PDX models were considered as separate tumors and scored individually for both paclitaxel (Fig. 5a) and eribulin (Fig. 5b) sensitivity. Next, the percentage of correct scoring within each model was assessed and the reproducibility of the test was calculated. The REMIT assay was calculated to

have 80% reproducibility for paclitaxel, and 83% for eribulin testing. For paclitaxel, the reproducibility of the assay based on the in vivo and ex vivo correlation was additionally calculated and scored at 70% (Fig. 5c).

**Discussion**

In this study, the REMIT assay was further developed and validated to assess ex vivo sensitivity to paclitaxel and eribulin in BC. The paclitaxel assay was validated with in vivo response in mice for all ten tested models, showing 90% correlation. The novel eribulin assay was developed using the same PDX models, out of which one model was tested for eribulin sensitivity in vivo, which was used as a representative model for assay development. Out of the ten tested models, seven showed overlap in the sensitivity to both paclitaxel and eribulin.

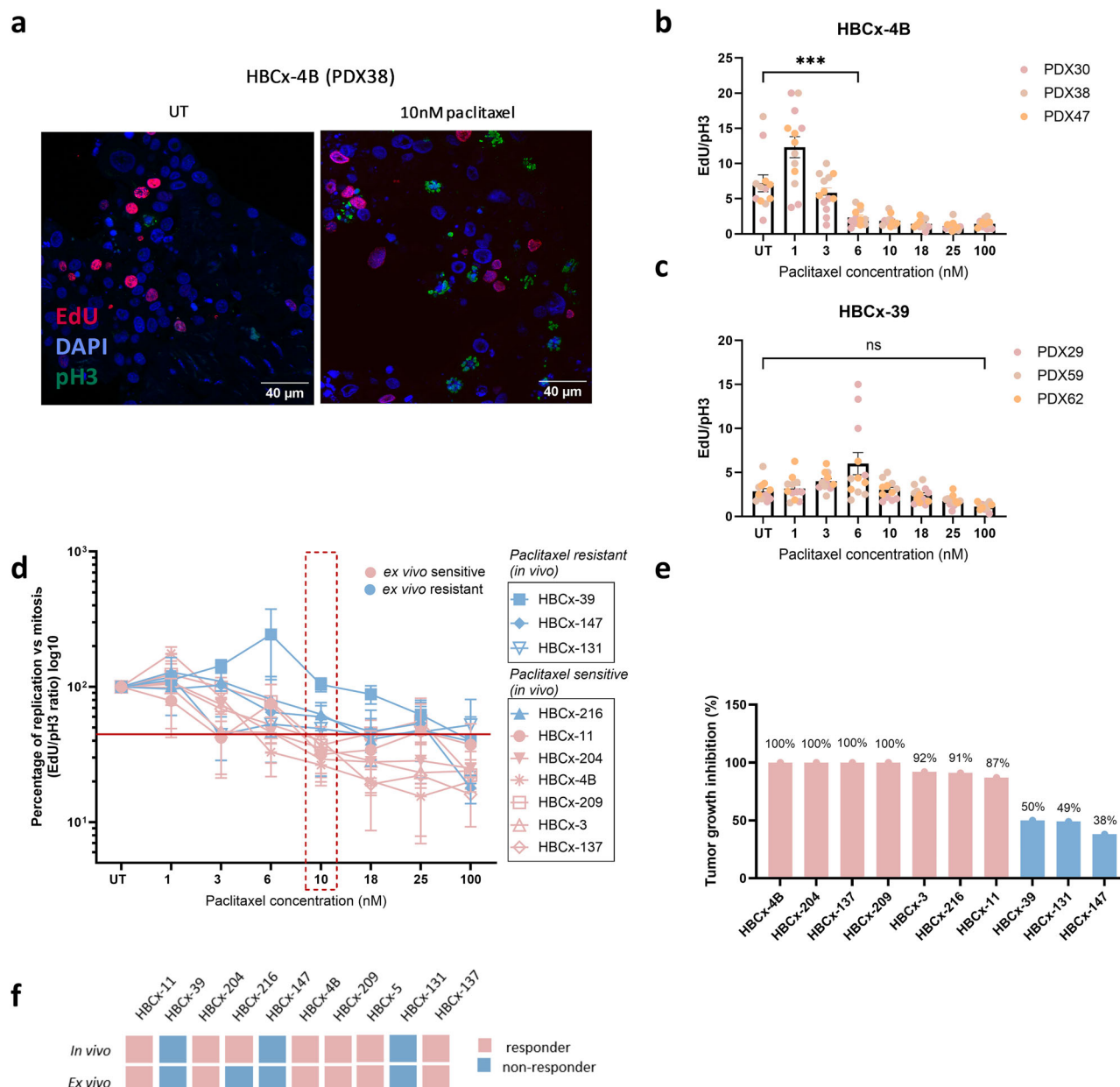


**Fig. 2 | Paclitaxel sensitivity assessed by the REMIT assay.** **a** Confocal image of the DAPI (blue), pH3 (green) and EdU (pink) immunostaining showing an increase in the number of mitotic cells after paclitaxel treatment in HBCx-4B. EdU/pH3 ratios of HBCx-4B (**b**; paclitaxel-sensitive) and HBCx-39 (**c**; paclitaxel-resistant), experiments performed in triplicate. Each data point represents a microscopic field of view analyzed, with 3–5 fields of view measured per replicate. Error bars represent the SEM, significance of the differences is indicated with significant results showed with stars and non-significant with ns. **d** EdU/pH3 ratios normalized to the control

sample of all tested PDX models, representing the thresholds applied to distinguish between sensitive and resistant models. All models were tested in  $n=3$  for all concentrations, except of HBCx-137 were the concentration of 1 and 25 nM of paclitaxel was included in  $n=2$ . Error bars represent the SEM. **e** Results of the tumor growth inhibition in mice in vivo after treatment with paclitaxel. Models are categorized between sensitive and resistant based on the percentage of TGI. **f** Schematic overview of the ex vivo paclitaxel sensitivity results and their concordance with the in vivo sensitivity tested in mice.

To meet the pressing clinical need for functional assays for chemotherapy response prediction, we aimed to extend the previously developed sensitivity tests<sup>10,11</sup> with a paclitaxel sensitivity assay. As indicated, the concentration range used for paclitaxel sensitivity testing was based on the docetaxel sensitivity assay described in our previous study<sup>11</sup> (1–100 nM), with addition of intermediate concentrations (3, 6, 18 and 25 nM). Direct comparison of these concentrations to paclitaxel levels achieved in patients is challenging due to differences between the in vivo drug bioavailability and the ex vivo exposure to the treatment. Different clinical studies report various maximal plasma levels ( $C_{max}$ ) that can be achieved in patients, mostly in the micromolar range<sup>21,22</sup>. Nevertheless, the levels achieved after the peak concentration return to the range applied in this study within

24 hours<sup>23</sup>. As the block in mitosis is expected to be reversible when paclitaxel concentrations drop, the levels over a more extended period might be the most relevant parameter for the effect in the patient. Therefore, we believe that the range of 1–100 nM paclitaxel has relevance for the in vivo situation.

We did not find a clear effect of paclitaxel on the survival of tested PDX tumors, confirming that paclitaxel treatment does not lead to cell death induction in the tissue slices cultured ex vivo within the three days of the experiment. This is in line with other findings in which the effect of paclitaxel treatment seems to vary between models, showing cell death induction in cell lines<sup>24,25</sup> and no clear effect in ex vivo cultures<sup>26</sup>. To adapt the sensitivity assay to the ex vivo culture, we developed an alternative method to

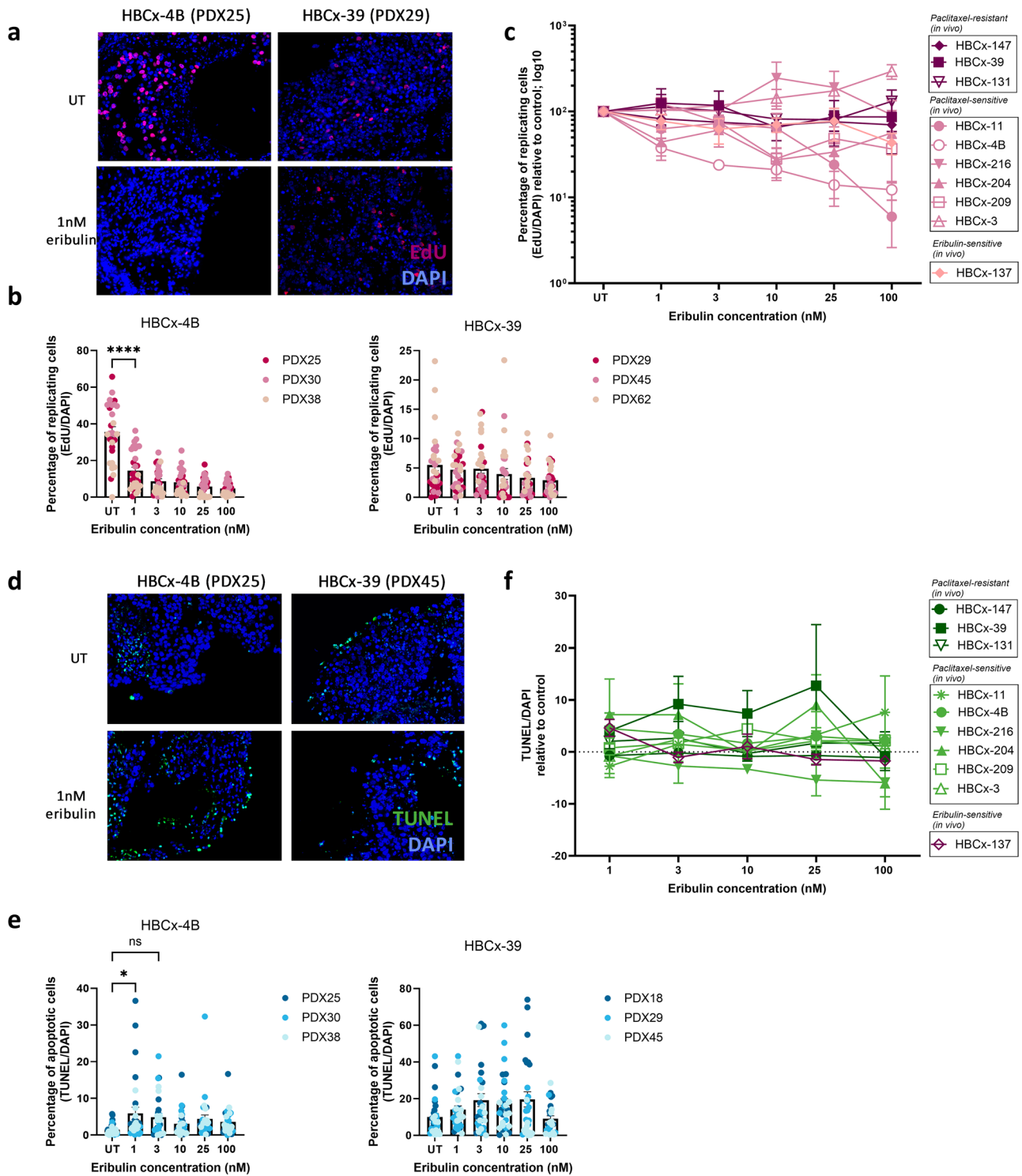


**Fig. 3 | Viability levels of PDX tissue slices after eribulin treatment.** **a** Microscopic images of EdU (pink) and DAPI (blue) channels for two selected models: HBCx-4B and HBCx-39. **b** Quantification of HBCx-4B and HBCx-39 proliferation. Each data point represents quantification of the percentage of EdU positive cells within one microscopic field of view; ten fields of view were analyzed per condition in triplicate. Error bars represent SEM. **c** Combined results of the EdU/DAPI percentage normalized to the untreated sample for each model separately. Error bars represent

SEM. **d** Microscopic images of TUNEL (green) and DAPI (blue) channels for two selected models: HBCx-4B and HBCx-39. **e** Quantification of HBCx-4B and HBCx-39 TUNEL staining. Each data point represents quantification of the percentage of cells in apoptosis within one microscopic field of view; ten fields of view were analyzed per condition in triplicate. Error bars represent SEM. **f** Combined results of the TUNEL/DAPI percentage normalized by subtracting the TUNEL levels from the untreated sample for each model separately. Error bars represent SEM.

predict taxane sensitivity by measuring cells inhibited in mitosis<sup>11</sup>. Here, we validated this sensitivity assay by measuring the ratio between replication and mitosis (EdU/pH3), and comparing it with the in vivo response determined in mice. The concordance between the ex vivo and in vivo

paclitaxel sensitivity reached 90%, confirming this to be a suitable functional test for treatment outcome prediction. Out of the ten tested models, only one PDX (HBCx-216) showed a clear difference in response, being sensitive to paclitaxel in vivo, but resistant ex vivo. This difference could be explained by

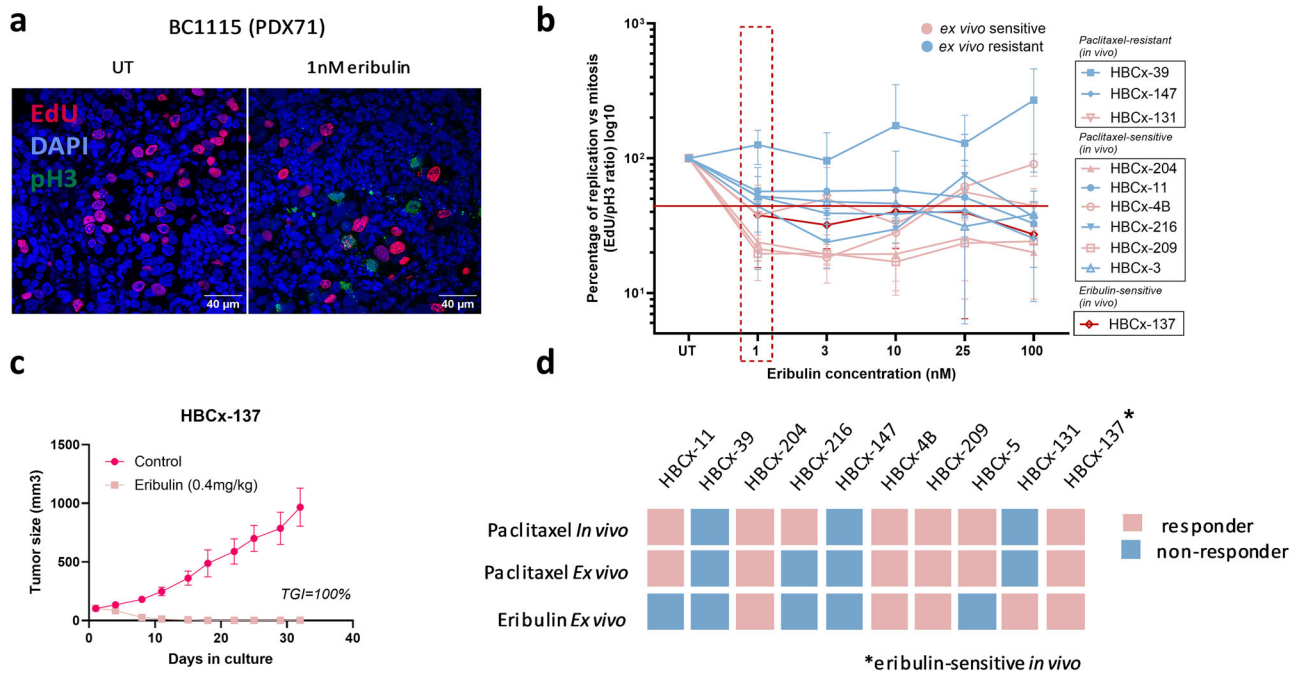


**Fig. 4 | Eribulin sensitivity assessment using the REMIT assay.** **a** Representative images of the pH3- (green) and EdU-positive (pink) cells with and without eribulin treatment for the HBCx-137 PDX model (eribulin-sensitive in vivo). **b** EdU/pH3 results normalized to the untreated samples of all tested PDX models, representing the thresholds applied to distinguish between sensitive and resistant models after treatment with 1 nM of eribulin. Models represented in the graph were treated in triplicate (except for HBCx-216 at 25 nM, and HBCx-209 at 25 and 100 nM, both

treated twice). Error bars represent the SEM. **c** Results of the in vivo eribulin treatment of the HBCx-137 PDX model, representing the measurements of the tumor size in mm<sup>3</sup> over the time in culture. Error bars represent the SEM. **d** Schematic overview of the ex vivo and in vivo paclitaxel sensitivity results and their correlation with the ex vivo sensitivity to eribulin. The average response combined from triplicate results is represented. The in vivo sensitivity to eribulin is known for the HBCx-137 model, as depicted in the figure.

a significant increase in the levels of replication observed after paclitaxel treatment in the HBCx-216 model (Supplementary Fig. 2b). This directly results in a higher EdU/pH3, regardless of changes in the levels of mitosis. For that reason, these two read-outs (EdU/pH3 and EdU/DAPI) should always be performed in parallel to exclude false-negative scoring. When moving forward to a clinical setting, this phenomenon should be further investigated and if increased levels of replication are detected in a significant number of tested samples, the method may have to be adjusted.

To extend our ex vivo chemotherapy response sensitivity assay we included eribulin treatment in the tested group of PDXs. Out of ten models included in the study, only the HBCx-137 model was tested in mice in vivo and scored sensitive for eribulin sensitivity. To select the most optimal read-out for eribulin, the levels of replication (EdU/DAPI), apoptosis (TUNEL) and relative mitosis (EdU/pH3) were assessed after the treatment. Similarly to paclitaxel treatment, no changes in the tumor cells survival that could be used for sensitivity assay were observed. The EdU/pH3 assay showed more pronounced differences among the models. Moreover, the in vivo eribulin-sensitive model HBCx-137 showed sensitivity to the treatment based on the EdU/pH3 read-out, validating the accuracy of the test. The EdU/pH3 test was chosen to categorize the models between ex vivo sensitive and resistant. As eribulin treatment is often used in patients with the initial response to paclitaxel<sup>20,27</sup>, we were interested to see whether any overlap in the sensitivity to paclitaxel and eribulin can be observed. We showed that seven out of ten tested models showed the same sensitivity to both treatments. Three out of ten tested models showed differences in the response to paclitaxel and eribulin, which is in line with a phase II clinical study where no correlation between the sensitivity to taxanes and response to eribulin was observed<sup>28</sup>. Considering that only one of the ten models used in this study was tested for the in vivo sensitivity to eribulin, the results presented in this report should be further confirmed in another PDX-based or clinical proof-of-concept study.

Although both paclitaxel and eribulin are chemotherapeutics that affect the function of microtubules, there are differences in their mechanism

of action. Paclitaxel promotes the assembly of alpha and beta tubulin by binding to the microtubules, which in turn stabilizes them and disrupts cell division<sup>29</sup>. Eribulin, on the other hand, can bind to a unique site on the tubulin that results in a suppression of microtubule polymerization and sequestration of the tubulin into non-productive tubulin aggregates<sup>30</sup>. Due to the differences in the mechanism of action of these chemotherapeutics, eribulin is often used in the clinic for patients with paclitaxel resistance acquired during the treatment regimen. The EdU/pH3 assay could be used to predict the response to eribulin in the group of refractory patients<sup>28,31</sup>, to determine the potential of the treatment.

To determine the potential of the paclitaxel and eribulin assays the reproducibility was assessed and scored around 80%. The differences between replicates can partially be explained by the inter-tumor heterogeneity, which was also observed in the in vivo response to the treatment (Supplementary Fig. 4a). Models with a homogenous sensitivity to paclitaxel in vivo (HBCx-4B, HBCx-209 and HBCx-204), mostly showed analogous consistent sensitivity ex vivo (HBCx-4B and HBCx-204). The heterogeneity in one of the replicates of the HBCx-209 model (PDX61) may be explained by the EdU/pH3 values after treatment of this tumor that were close to the threshold border (48.9%). This confirms the robustness of the assay in positive scoring of paclitaxel-sensitive samples. Overall, we consider the reproducibility of the assay positive, considering the general heterogeneity present in the tumor models, however it should be re-assessed when moving towards a clinical setting in a proof-of-concept clinical study using fresh biopsy material derived from patients. The thresholds applied in the current study might have to be adjusted for the clinical setting, as the current threshold has been set using the PDX models. Furthermore, additional factors will influence the treatment response in patient material. The main challenge that can be encountered during the validation of the paclitaxel and eribulin assays in patient material is that the sample size is too small to catch heterogeneity between patients. Moreover, human components of the tumor microenvironment, including T- and B-cells missing in the PDX models, are present in patient material samples. Paclitaxel treatment has

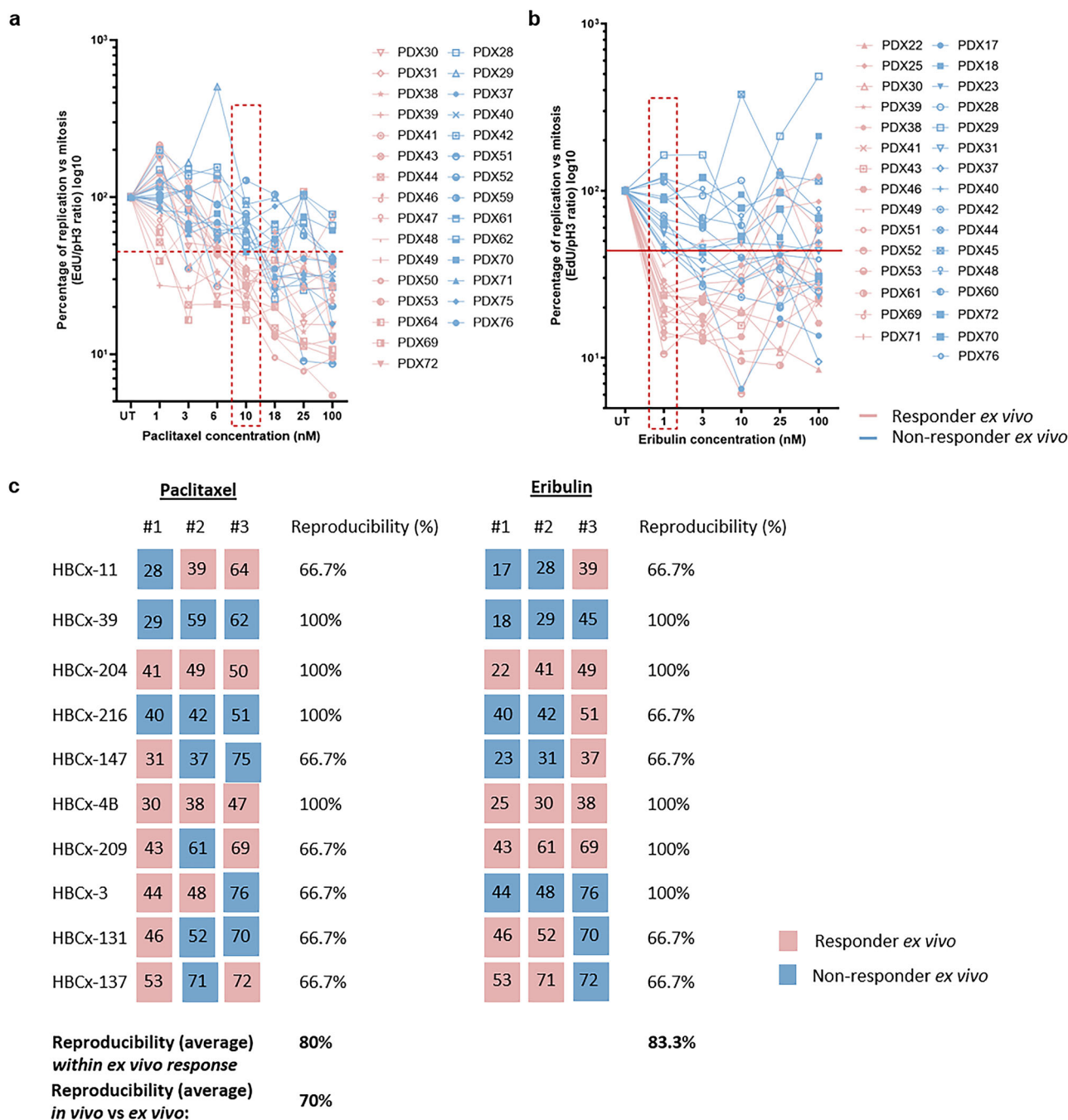


**Fig. 5 | Reproducibility of the REMIT assay for paclitaxel and eribulin sensitivity assessment.** All replicates from the tested PDX models plotted and scored separately for paclitaxel (a) and eribulin (b) sensitivity. Thresholds applied in the graphs are the same as depicted in Figs. 2 and 4, respectively. Blue lines represent replicates scored as resistant to paclitaxel and pink as sensitive to paclitaxel treatment. c Schematic overview of the scoring performed for each

of the PDX replicates separately with the division between the models. Calculations represent the reproducibility of the assay for each models separately and an average value for paclitaxel and eribulin assay. For paclitaxel, the reproducibility based on the correlation between in vivo and ex vivo sensitivity was also calculated. Numbers within the colored squares represent the PDX replicate included in the analysis.

been shown to enhance anti-tumor response of the immune system in different ex vivo and in vivo models<sup>32,33</sup> and was observed to increase the number of tumor-infiltrating lymphocytes in BC patients<sup>34</sup>. Therefore, the presence of the human tumor microenvironment can aid to better elucidate the systematic response of cancer cells to the treatment. All these factors should be taken into consideration during the initiation and assessment of the clinical validation trial for paclitaxel and eribulin sensitivity assays. Based on the preliminary data using primary breast cancer resection material (supplementary Fig. 5) and our previous work, we believe that these

challenges can in principle be met without any changes to the protocols described here<sup>10</sup>.

In this study, two new ex vivo chemotherapy sensitivity assays were developed and validated in PDX tumors with known in vivo sensitivity to paclitaxel and eribulin. As no direct tumor killing was observed for both treatments ex vivo, the REMIT assay was determined to be the most suitable to accurately predict treatment outcome. The reproducibility of the REMIT assay was scored 80% for paclitaxel and 83% for eribulin, showing great potential for further clinical validation.

**Table 1 | Characteristics of the PDX models used in the study**

PDX model	BC subtype	Origin	Mutation	Reference
HBCx-3	ER+	primary tumor	<i>TP53</i> mut., <i>PTEN</i> del.	19
HBCx-4B	TNBC	metastasis (lymph node)	<i>PIK3CA</i> , <i>TP53</i> and <i>NF1</i> mut.	21
HBCx-11	TNBC	primary tumor	<i>BRCA1</i> and <i>TP53</i> mut.	19
HBCx-39	TNBC	residual tumor	<i>TP53</i> mut.	21
HBCx-131	ER+	metastasis (bone)	<i>FGFR1</i> and <i>CCND1</i> amp.; <i>CDKN2A</i> del.	22
HBCx-137	ER+	metastasis (bone)	<i>GATA3</i> mut.; <i>FGFR1</i> , <i>FGFR2</i> , <i>PAK1</i> and <i>CCND1</i> amp.; <i>CCNE2</i> del.	22
HBCx-147	TNBC	residual tumor	-	20
HBCx-204	TNBC	residual tumor	<i>TP53</i> and <i>NOTCH1</i> mut.	21
HBCx-209	TNBC	residual tumor	<i>BRCA1</i> and <i>TP53</i> mut.; <i>CDKN2A/CDKN2B</i> del.	21
HBCx-216	TNBC	local relapse	<i>TP53</i> mut.; <i>CDKN2A/CDKN2B</i> and <i>PTEN</i> del.	not published yet

## Methods

### Patient-derived Xenografts and BC resection material

Ten different patient-derived xenografts (PDXs) of BC were established at the Institut Curie in Paris (Table 1), as described previously<sup>35–37</sup>. Paclitaxel and eribulin were administered at 20 or 25 mg/kg weekly by IP, and at 0.4 mg/kg weekly by IV, respectively. Tumor growth was evaluated by measuring two perpendicular tumor diameters with calipers twice weekly. Individual tumor volumes were estimated using two diameters *a* and *b* for simplification, as follows:  $TV = (a \times b^2)/2$ , where “*a*” is the largest diameter, and “*b*” is the smallest diameter. Tumor growth inhibition (TGI) was assessed by dividing median TV in the treated group by median TV in the control group at the same time ( $TGI = 100 - TV_{\text{treated}} \times 100 / TV_{\text{control}}$ )<sup>35</sup>. Tumors were considered sensitive to treatment when the TGI was above 80%, intermediate between 50% and 80%, and resistant below 50%. PDX models included in this study consisted of seven paclitaxel sensitive and three resistant tumors.

Residual primary breast cancer tissue was prospectively collected from patients undergoing wide local excision or ablation at the Erasmus MC Cancer Institute and Maasstad Hospital in Rotterdam, The Netherlands. Following the macroscopic evaluation of the surgical specimens by pathologists, fresh residual tumor tissue was collected for research purposes in compliance with the Code of Proper Secondary Use of Human Tissue in the Netherlands, established by the Dutch Federation of Medical Scientific Societies. This study was conducted in accordance with the ethical principles outlined in the Declaration of Helsinki. The need for written informed consent has been waived by the ethical committee, and patients who objected to the secondary use of residual tumor material for research were excluded from the study. This protocol was approved by the Erasmus MC Medical Ethics Commission (MEC-11-098).

### Tumor Slicing, Handling and Drug Treatment Ex Vivo

BC PDX tissue samples were collected and preserved in customized breast medium, as previously described<sup>38</sup>. The PDXs tumors measured approximately 15 × 15 mm (+/– 2 mm) upon collection, corresponding to the final tumor volume observed in the *in vivo* experiments. The samples were then transported overnight on ice, which maintained the viability of the tumors (see Supplementary Fig. 1). Upon arrival, the PDX tumors were sliced using a Leica VT 1200S Vibratome (Leica Microsystems, Wetzlar, Germany). Tumors were embedded in 4% low melting agarose in PBS and 300 μm thick slices were generated. The tissue slices were subsequently cultured in customized breast medium at 37 °C in a 5% CO<sub>2</sub> humidified incubator with continuous rotation (60 rpm) provided by a Stuart SSM1 mini orbital shaker (Camlab Ltd, Cambridge, UK).

To develop the drug-sensitivity assay, ten different PDX models were tested in triplicate for each chemotherapy concentration. The PDX tissue slices were treated with a range of concentrations of paclitaxel: 1, 3, 6, 10, 18, 25, and 100 nM (Sigma-Aldrich, St. Louis, MO, USA). These concentrations were selected based on the

previously used concentrations of docetaxel in the study performed by Ladan et al.<sup>11</sup>. Docetaxel and paclitaxel are chemotherapeutics with a similar mechanism of action<sup>39,40</sup>, however docetaxel has been shown to be more potent than paclitaxel<sup>41</sup>, with example concentrations in the clinical setting of 95 mg/m<sup>2</sup> for docetaxel and 173 mg/m<sup>2</sup> for paclitaxel<sup>42</sup>. Taking these values into account, we decided to use a comparable concentration range for paclitaxel testing as the one used in the docetaxel study<sup>11</sup> (1–100 nM), and include additional intermediate concentrations (3, 6, 18 and 25 nM). As eribulin has previously been used in a similar concentration range to paclitaxel, but showed a higher potency of the treatment<sup>43</sup>, for better comparison between the treatments in our set up analogous concentrations were used consisting of 1, 3, 10, 25, and 100 nM (MedChemExpress LLC, Monmouth Junction, NJ, USA). The slices were then incubated for three days. To evaluate cell replication, 30 μM 5-Ethynyl deoxyuridine (EdU) (Invitrogen, Carlsbad, CA, USA) was added to the culture medium 2 hours before fixation. Following the incubation period, the tissue slices were fixed in 10% neutral buffered formalin for 24–72 hours at room temperature. Subsequently, the tissue was embedded in paraffin, and 4 μm sections were obtained for further analysis.

### Immunostaining, image acquisition, and analysis

Immunostainings were performed for tissue replication, mitosis and apoptosis. For cell replication, a chemical click-it reaction was performed with Atto 594 (Invitrogen, Waltham, MA, USA) to visualize incorporated EdU molecules, as described before<sup>38</sup>. Cells in mitosis were visualized using the anti-phospho serine10 histone H3 antibody (pH3; 1/100 dilution) (Merck Millipore, Burlington, MA, USA) and the secondary Goat anti-Rabbit Alexa Fluor 488 (1/1000 dilution) (Thermo Fisher Scientific, Waltham, MA, USA) as previously described<sup>11</sup>. The pH3 and EdU stainings were combined and carried out simultaneously. To observe cells in apoptosis a terminal deoxynucleotidyl transferase dUTP nick end-labeling (TUNEL; In situ Cell Death Detection Kit; Roche Diagnostics, Basel, Switzerland) assay was performed, as described previously<sup>38</sup>. To visualize cell proliferation the monoclonal mouse anti-human antigen Ki67 antibody (clone MIB-1; M7240) (Agilent DAKO, Santa Clara, CA, USA) was used in combination with the secondary Goat anti-Mouse Alexa Fluor 488 (1/1000 dilution) (Thermo Fisher Scientific, Waltham, MA, USA).

Microscopic images were acquired using the Automated Upright Microscope Leica DM4000 B with a magnification of 200x (Leica Microsystems, Wetzlar, Germany). If possible, ten fields of view were imaged per condition. In the case of a small sample size, a minimum of six fields of view were acquired. Images were subsequently analyzed using the ImageJ software on the basis of a total number of pixels from red channel (EdU), the green channel (TUNEL) and the

blue channel (DAPI). Next, the percentage of the EdU or TUNEL signal was calculated out of the total of the DAPI signal. For the analysis of the number of pH3- and EdU-positive cells, a manual quantification was performed. Four fields of view were analyzed per condition by counting the number of pH3-positive (mitotic) and EdU-positive (replicating) nuclei.

### Statistics

The acquired data was statistically analyzed using Graph Pad Prism® version 9. A standard two-way ANOVA test was used together with Tukey's multiple comparison test. *P*-values below 0.05 were considered significant. Unless stated otherwise, all experiments were performed in triplicate.

### Data availability

The authors declare that the data supporting the findings of this study are available within the paper and its supplementary information files. Any additional information is available from the corresponding author upon reasonable request.

### Code availability

For the analysis of the number of red or green pixels from a total of blue pixels (EdU or TUNEL out of DAPI signal) a macro was made for the ImageJ software. Any additional information regarding the script is available from the corresponding author upon reasonable request.

Received: 7 August 2024; Accepted: 4 February 2025;

Published online: 17 February 2025

### References

1. WHO. WHO launches new roadmap on breast cancer, <<https://www.who.int/news/item/03-02-2023-who-launches-new-roadmap-on-breast-cancer>> (2023).
2. Onitilo, A. A., Engel, J. M., Greenlee, R. T. & Mukesh, B. N. Breast cancer subtypes based on ER/PR and Her2 expression: comparison of clinicopathologic features and survival. *Clin. Med. Res.* **7**, 4–13 (2009).
3. Mohamed, A., Krajewski, K., Cakar, B. & Ma, C. X. Targeted therapy for breast cancer. *Am. J. Pathol.* **183**, 1096–1112 (2013).
4. Spring, L. et al. (American Society of Clinical Oncology, 2022).
5. Carlino, F. et al. Immune-based therapy in triple-negative breast cancer: from molecular biology to clinical practice. *Cancers* **14**, 2102 (2022).
6. Li, Y. et al. Recent advances in therapeutic strategies for triple-negative breast cancer. *J. Hematol. Oncol.* **15**, 121 (2022).
7. Gradishar, W. J. et al. Breast cancer, version 3.2022, NCCN clinical practice guidelines in oncology. *J. Natl Compr. Cancer Netw.* **20**, 691–722 (2022).
8. Shien, T. & Iwata, H. Adjuvant and neoadjuvant therapy for breast cancer. *Jpn. J. Clin. Oncol.* **50**, 225–229 (2020).
9. Barzaman, K. et al. Breast cancer: Biology, biomarkers, and treatments. *Int. Immunopharmacol.* **84**, 106535 (2020).
10. Ladan, M. M. et al. Proof-of-concept study linking ex vivo sensitivity testing to neoadjuvant anthracycline-based chemotherapy response in breast cancer patients. *NPJ Breast Cancer* **9**, 80 (2023).
11. Ladan, M. M. et al. Functional ex vivo tissue-based chemotherapy sensitivity testing for breast cancer. *Cancers* **14**, 1252 (2022).
12. Gradishar, W. J. et al. Phase II trial of nab-paclitaxel compared with docetaxel as first-line chemotherapy in patients with metastatic breast cancer: final analysis of overall survival. *Clin. breast cancer* **12**, 313–321 (2012).
13. Jordan, M. A., Toso, R. J., Thrower, D. & Wilson, L. Mechanism of mitotic block and inhibition of cell proliferation by taxol at low concentrations. *Proc. Natl Acad. Sci.* **90**, 9552–9556 (1993).
14. Schiff, P. B. & Horwitz, S. B. Taxol stabilizes microtubules in mouse fibroblast cells. *Proc. Natl Acad. Sci.* **77**, 1561–1565 (1980).
15. Xiao, H. et al. Insights into the mechanism of microtubule stabilization by Taxol. *Proc. Natl Acad. Sci.* **103**, 10166–10173 (2006).
16. Pizzuti, L. et al. Eribulin in triple negative metastatic breast cancer: critic interpretation of current evidence and projection for future scenarios. *J. Cancer* **10**, 5903 (2019).
17. O'Shaughnessy, J. et al. Efficacy of eribulin for metastatic breast cancer based on localization of specific secondary metastases: a post hoc analysis. *Sci. Rep.* **10**, 11203 (2020).
18. Jordan, M. A. et al. The primary antimetabolic mechanism of action of the synthetic halichondrin E7389 is suppression of microtubule growth. *Mol. Cancer Ther.* **4**, 1086–1095 (2005).
19. Long, B. H. & Fairchild, C. R. Paclitaxel inhibits progression of mitotic cells to G1 phase by interference with spindle formation without affecting other microtubule functions during anaphase and telephase. *Cancer Res.* **54**, 4355–4361 (1994).
20. Lorusso, V. et al. Efficacy and safety of eribulin in taxane-refractory patients in the 'real world'. *Future Oncol.* **13**, 971–978 (2017).
21. Huizing, M. T. et al. Pharmacokinetics of paclitaxel and three major metabolites in patients with advanced breast carcinoma refractory to anthracycline therapy treated with a 3-hour paclitaxel infusion: a European Cancer Centre (ECC) trial. *Ann. Oncol.* **6**, 699–704 (1995).
22. Stage, T. B., Bergmann, T. K. & Kroetz, D. L. Clinical pharmacokinetics of paclitaxel monotherapy: an updated literature review. *Clin. Pharmacokinet.* **57**, 7–19 (2018).
23. Lee, H. J. et al. A phase I study of oral paclitaxel with a novel P-glycoprotein inhibitor, HM30181A, in patients with advanced solid cancer. *Cancer Res. Treat.* **46**, 234 (2014).
24. Khing, T. M. et al. The effect of paclitaxel on apoptosis, autophagy and mitotic catastrophe in AGS cells. *Sci. Rep.* **11**, 23490 (2021).
25. Ling, Y.-H., Yang, Y., Tornos, C., Singh, B. & Perez-Soler, R. Paclitaxel-induced apoptosis is associated with expression and activation of c-Mos gene product in human ovarian carcinoma SKOV3 cells. *Cancer Res.* **58**, 3633–3640 (1998).
26. Urbaniak, A., Piña-Oviedo, S., Yuan, Y., Huczynski, A. & Chambers, T. C. Limitations of an ex vivo breast cancer model for studying the mechanism of action of the anticancer drug paclitaxel. *Eur. J. Pharmacol.* **891**, 173780 (2021).
27. Jeong, Y. G. et al. Combined PI3K inhibitor and eribulin enhances anti-tumor activity in preclinical models of paclitaxel-resistant, PIK3CA-mutated endometrial cancer. *Cancers* **15**, 4887 (2023).
28. Inoue, K. et al. Phase II clinical study of eribulin monotherapy in Japanese patients with metastatic breast cancer who had well-defined taxane resistance. *Breast Cancer Res. Treat.* **157**, 295–305 (2016).
29. Abu Samaan, T. M., Samec, M., Liskova, A., Kubatka, P. & Büsselberg, D. Paclitaxel's mechanistic and clinical effects on breast cancer. *Biomolecules* **9**, 789 (2019).
30. Dabydeen, D. A. et al. Comparison of the activities of the truncated halichondrin B analog NSC 707389 (E7389) with those of the parent compound and a proposed binding site on tubulin. *Mol. Pharmacol.* **70**, 1866–1875 (2006).
31. Kuznetsov, G., TenDyke, K., Yu, M. & Littlefield, B. Antiproliferative effects of halichondrin B analog eribulin mesylate (E7389) against paclitaxel-resistant human cancer cells in vitro. *Mol. Cancer Ther.* **6**, C58–C58 (2007).
32. Vicari, A. P. et al. Paclitaxel reduces regulatory T cell numbers and inhibitory function and enhances the anti-tumor effects of the TLR9 agonist PF-3512676 in the mouse. *Cancer Immunol., Immunother.* **58**, 615–628 (2009).
33. Hu, Y. et al. Paclitaxel induces micronucleation and activates pro-inflammatory cGAS–STING signaling in triple-negative breast cancer. *Mol. Cancer Ther.* **20**, 2553–2567 (2021).
34. Demaria, S. et al. Development of tumor-infiltrating lymphocytes in breast cancer after neoadjuvant paclitaxel chemotherapy. *Clin. Cancer Res.* **7**, 3025–3030 (2001).

35. Marangoni, E. et al. A new model of patient tumor-derived breast cancer xenografts for preclinical assays. *Clin. Cancer Res.* **13**, 3989–3998 (2007).
36. Coussy, F. et al. A large collection of integrated genomically characterized patient-derived xenografts highlighting the heterogeneity of triple-negative breast cancer. *Int. J. Cancer* **145**, 1902–1912 (2019).
37. El-Botty, R. et al. Oxidative phosphorylation is a metabolic vulnerability of endocrine therapy and palbociclib resistant metastatic breast cancers. *Nat. Commun.* **14**, 4221 (2023).
38. Naipal, K. A. T. et al. Tumor slice culture system to assess drug response of primary breast cancer. *BMC Cancer* **16**, 1–13 (2016).
39. Saloustros, E., Mavroudis, D. & Georgoulas, V. Paclitaxel and docetaxel in the treatment of breast cancer. *Expert Opin. Pharmacother.* **9**, 2603–2616 (2008).
40. Horwitz, S. B. Taxol (paclitaxel): mechanisms of action. *Ann. Oncol.* **5**, S3–S6 (1994).
41. Verweij, J., Clavel, M. & Chevalier, B. Paclitaxel (Taxol™) and docetaxel (Taxotere™): Not simply two of a kind. *Ann. Oncol.* **5**, 495–505 (1994).
42. Jones, S. E. et al. Randomized phase III study of docetaxel compared with paclitaxel in metastatic breast cancer. *J. Clin. Oncol.* **23**, 5542–5551 (2005).
43. Towle, M. J. et al. In vitro and in vivo anticancer activities of synthetic macrocyclic ketone analogues of halichondrin B. *Cancer Res.* **61**, 1013–1021 (2001).

### Acknowledgements

We thank Mieke Bavelaar for expert help with some experiments. This project was funded by the Dutch Cancer Foundation (KWF 13651) and the Oncode Institute, which is partly financed by the Dutch Cancer Foundation. The funders played no role in study design, data collection, analysis and interpretation of data, or writing the paper.

### Author contributions

Study conception and design were done by D.v.G. and A.J. Data collection from the experiments performed on PDX models and gathering of the PDX tumor material was performed by E.M, A.D and E.M. Preparation of the PDX material, the ex vivo data collection and analysis was performed by Z.M.K.

and N.S.V. The first draft of the paper was written by Z.M.K and D.v.G. and all authors commented on previous versions of the paper. All authors read and approved the final paper.

### Competing interests

The authors declare no competing interests.

### Additional information

**Supplementary information** The online version contains supplementary material available at

<https://doi.org/10.1038/s41523-025-00734-x>.

**Correspondence** and requests for materials should be addressed to Dik C. van Gent.

**Reprints and permissions information** is available at

<http://www.nature.com/reprints>

**Publisher's note** Springer Nature remains neutral with regard to jurisdictional claims in published maps and institutional affiliations.

**Open Access** This article is licensed under a Creative Commons Attribution-NonCommercial-NoDerivatives 4.0 International License, which permits any non-commercial use, sharing, distribution and reproduction in any medium or format, as long as you give appropriate credit to the original author(s) and the source, provide a link to the Creative Commons licence, and indicate if you modified the licensed material. You do not have permission under this licence to share adapted material derived from this article or parts of it. The images or other third party material in this article are included in the article's Creative Commons licence, unless indicated otherwise in a credit line to the material. If material is not included in the article's Creative Commons licence and your intended use is not permitted by statutory regulation or exceeds the permitted use, you will need to obtain permission directly from the copyright holder. To view a copy of this licence, visit <http://creativecommons.org/licenses/by-nc-nd/4.0/>.

© The Author(s) 2025